FACULTY 1: PHYSICS AND ELECTRICAL ENGINEERING
INSTITUTE FOR ARTIFICIAL INTELLIGENCE

MASTER THESIS (INFORMATION AND AUTOMATION ENGINEERING)

PARAMETERIZATION OF A CONSTRAINT-BASED AND OPTIMIZATION-BASED ROBOTIC MOTION CONTROLLER FOR OBJECTS GRASPING IN TABLE-TOP SCENARIOS

WRITTEN BY
MINERVA GABRIELA VARGAS GLEASON (3020449)
ON JULY 24, 2017

SUPERVISOR:	DR. ING. DANIJELA RISTIC-DURRANT
SUPERVISOR:	PROF. MICHAEL BEETZ PHD
RVIEWER:	REVIEWERS

*EXZELLENT.

Contents

List of Figures

CHAPTER 1

Introduction

1.1 Motivation

The number and applications of robots in our society is growing day by day, we can find them in production lines, at hospitals, as guides in museums and even at home, just to mention some examples. The capabilities and autonomy required by each robot widely varies depending on its application.

Most industrial robots used in assembly lines have no sensors that gives them information about their environment, they work by moving from one predefined position to the next one, executing controlled trajectories. Robots working without external information have to be kept in a controlled environment, where the position of all objects is known beforehand and they only have to execute a repetitive task.

Nowadays, service robots are envisioned to work in a wide range of situations where they dynamically interact with their environment, where the position of objects and obstacles is not known beforehand and can continuously change. Working under these conditions requires some degree of autonomy from the system.

The aim of this work is to develop the *motion generation component* of a *grasping system*

based on a whole-body motion controller. The system must be able to obtain a trajectory a robot has to execute in order to grasp a specified object. This implies generating a trajectory for a mechanical system with multiple degrees of freedom (DOFs) that successfully reaches a position and orientation under given conditions.

Object grasping and manipulation might seem trivial for humans, but it constitutes a big challenge in the robotics field. In order to successfully grasp an object, the robot must:

- Identify the object and its position with respect to the robot. This is done by a perception system which analyzes the information provided from sensors, normally cameras.
- Decide how to grasp the object. Usually, an object can be grasped in several ways. Taking a cup as example, it can be grabbed from the handle, from the cup body or from the top edge (figure 1.1). The system should be able to decide which one of this **grasping poses** is better depending on the situation.
- Generate and execute a trajectory that moves the end effector (EEF) from its current location to the selected grasping pose. This includes trajectory generation and motion control.

Being able to grasp an object is an essential ability in robot manipulation. Having a system that autonomously locates and grasp an object using *On-line Trajectory Generation (OTG)* gives great flexibility to the robot. OTG grants the capability of modifying the trajectory during execution, it implies recalculating the trajectory on every control cycle (in this case, around 1 msec). By doing this, the system is able to react instantaneously to unexpected events, such as a change in the goal position.

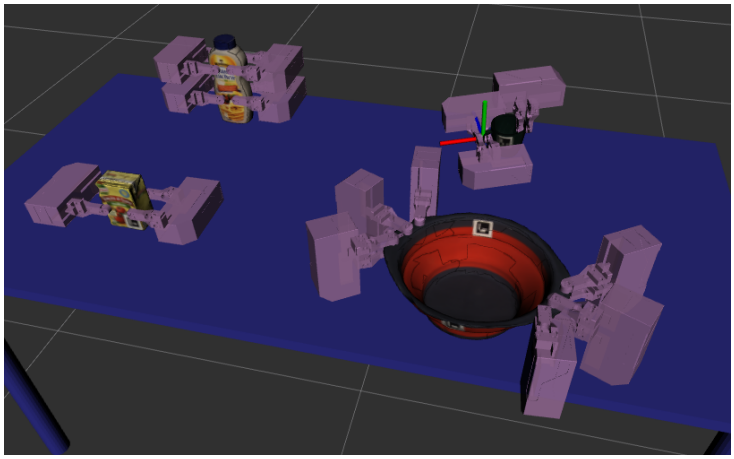

Figure 1.1: Example of objects with predefined grasping poses

The proposed solution to this grasping problem includes generating a data base of objects with predefined grasping poses (GP) (figure 1.1) and a perception system that detects the stored objects and shows the possible GP and it's position with respect to the robot.

The robot will have to decide which GP is better for grasping a specified object given a initial configuration. Then, a optimization controller (section 3.3) will generate several possible trajectories, evaluate them and send the best one to the robot.

1.2 Contributions

Data, software, algorithms, designs, etc... made by me If the problem was solved, how was that done?

1.3 Structure of the thesis

CHAPTER 2

Background & Related Job

This chapter presents the current state of the art of some relevant topics for mobile robotics that the reader needs to fully understand the content of this thesis. The first section will refer to mobile robots' localization.

2.1 Localization Algorithms (*if moving the base is required*)

Robot localization can be defined as the on-line estimation of a mobile robot's position based on sensor data; the position is given with respect to a global coordinate frame. Nowadays, localization is a fundamental research problem in robotics since it is required for most mobile robotics' tasks.

According to Fox et al. [1999b], the aim of *localization* is to estimate the position of a robot, given a map of the environment and data from the robot's sensors. Localization is often referred to as *position estimation*.

The current localization techniques can be separated on two groups according to the problem they solve ([Fox et al., 1999b]):

- **Tracking or local:** In this case, the initial position of the robot is known and the algorithm

only has to compensate for odometry errors that appear when the robot moves. The main problem they present is that they cannot recover if they lose track of the robot's position (considering some threshold).

- **Global:** These are able to obtain the initial position of a robot. In other words, they estimate the robot's position under global uncertainty. This is commonly known as the *wake-up robot problem*, where the initial location of the robot is unknown.

A well-known problem in robot localization is known as the *kidnapped robot problem*, where a robot is carried to a different location. Hence the robot must be able to determine whether the previous known position is wrong and,if it is, find its current location. Global algorithms are able to solve this problem.

2.1.1 Markov Localization (*if required*)

The *Markov Localization* is a global technique that estimates the position of the robot based on a probabilistic framework. Basically, what Markov localization does is represent the robot's belief by a probability distribution over possible positions [Fox et al., 1999a]. The belief is updated using Bayes rule every time the robot moves or receives data from its sensors.

Let us denote the robot's position by $l = (x, y, \theta)$, where x and y are the robot's coordinates with respect to a fixed world reference frame, and θ is the robot's orientation. The probability distribution that states the robot's belief of being at a certain position l is given by $Bel(l)$.

As shown in Figure 2.1, the robot starts with a uniform distribution of belief states representing that it is equally probable for the robot to be in any position in the environment. After receiving data from the sensors, the belief $Bel(l)$ is updated and the more probable positions

obtain a higher value. Eventually, the robot becomes highly certain about its position, which is represented by a narrow Gaussian distribution centered around the robot's current location.

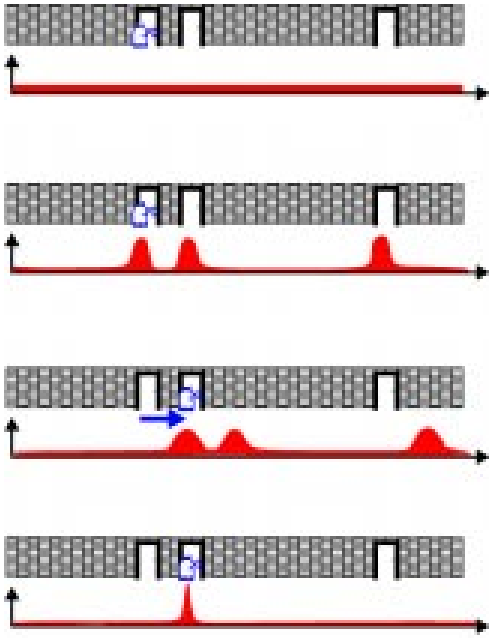

Figure 2.1: Markov localization: basic concept. [Fox et al., 1999b, chap. 2, page 393]

As explained by Fox et al. [1999a], the belief is updated with two different probabilistic models: a model that represents the robot's motion and a perception model that considers the sensor readings:

- **Robot motion:** The probability that a measured movement a occurs at a certain position l' is given by $P\ (l \mid l',\ a)$. This model is used to update the belief state every time a movement is executed.

$$Bel(l) \leftarrow \int P\ (l \mid l',\ a)\ Bel(\ l')\ dl' \tag{2.1}$$

- **Sensor readings:** The probability of receiving a sensor reading s when the robot is at the location l is given by $P\ (s \mid l)$. We can use this to update the robot's belief with:

$$Bel(l) \leftarrow \alpha\ P\ (s \mid l\ )\ Bel(l) \tag{2.2}$$

where α is a normalization factor that makes $Bel(l)$ integrate to 1.

Markov localization is able to globally estimate the position of the robot, recover from uncertainties and odometry errors and solve the kidnapped robot problem (re-localize the robot).

This localization technique uses a probability distribution over the space of all hypotheses of where the robot can be ($Bel(l)$) to estimate the current robot location. The computational resources needed to maintain this probability distribution for all possible positions increase with the size of the space. For normal environments, the required memory can easily exceed 100MB. The problem with the high computational cost also appears in *grid-based* Markov localization approaches, which discretize the relevant parts of the space using an evenly spaced grid of points.

This technique works under the assumption that the environment is static (*Markov assumption*), which is not true in some applications of mobile robotics. Sometimes, the robot can be located in an environment where it interacts with people and objects that can be moved. To solve the localization problem in this case, a different technique is required.

2.1.2 Monte Carlo Localization (*if required*)

Monte Carlo Localization (MCL) is a version of sampling-importance-resampling (SIR) based on Markov localization. It is a sample-based algorithm that uses particle filters to ensure the survival of the fittest.

According to Fox et al. [1999a], this algorithm uses fast sampling techniques to represent the robot's belief $Bel(l)$ by estimating the posterior distribution every time the robot moves or senses using the importance re-sampling technique.

MCL uses many samples during the global localization and the sample set size is significantly reduced during tracking when an approximate position of the robot is already known. Compared to grid-based Markov localization, MCL requires considerably less memory and, therefore, can integrate measurements at a higher frequency. It is more accurate and easier to implement than Markov localization. The main advantage MCL has is that it is able to perform *global localization*, meaning that MCL can obtain the initial position of a robot and solve the *kidnapped robot problem* at a low computational cost. This allows us to use MCL in bigger environments.

The key concept of this approach is to represent the posterior belief $Bel(l)$ by a set of N weighted, random particles $S = \{s_i \mid i = 1... N\}$. This sample set is a discrete approximation of a probability distribution. The distribution is updated by updating the weight of each particle after every sensor's reading or robot's movement.

The samples are represented by $\langle\langle x, y, \theta\rangle, p\rangle$, where the first three parameters denote a possible robot position and p is the weighting factor of the particle ($p \geq 0$). Assume $\sum_{n=1}^{N} p_n = 1$, all weights must be normalized so that they sum up to 1.

As explained by Fox et al. [1999a], updating the particle set is done in two different ways:

- **Robot Motion:** Every time the robot moves, N new samples are randomly created. These new samples approximate the robot's position with respect to the motion command. Each new sample is generated from the previous sample set with it's likelihood determined by the particle's weight. The location of the new sample is given by:

$$P(l \mid l', a) \tag{2.3}$$

  where a is the observed movement and l' the previous location. Figure 2.2 shows the behavior of this sampling technique where the robot starts with a known position and

moves following the straight lines.

The uncertainty of the sample sets increases with each iteration. This uncertainty represents the error in the robot's location due to slippage and drift.

- **Sensor readings:** The sample set is re-weighted implementing Bayes' rule. For a sample $\langle l, p \rangle$, the update rule is:

$$p \leftarrow \alpha P(s \mid l) \tag{2.4}$$

where s is the sensor information and α a normalization factor that ensures the weights satisfy $\sum_{n=1}^{N} p_n = 1$.

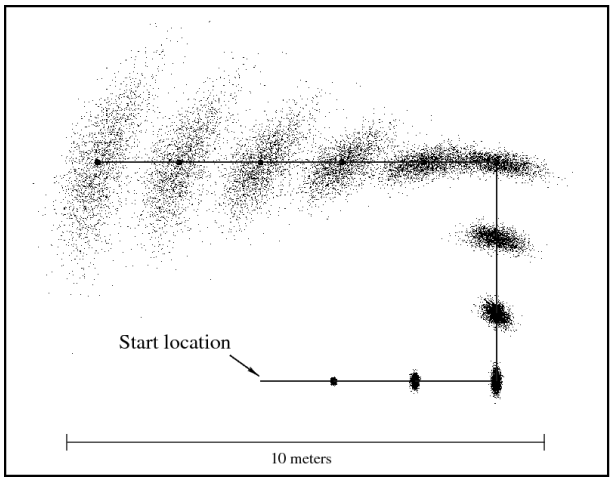

Figure 2.2: MCL approximation of the position's belief based only on motion commands [Fox et al., 1999a, page 3].

In every iteration, the sample set is centered around the robot's believed position, in case of an error in location (such as in the *kidnapped robot problem*, the robot wouldn't be able to re-localize itself. In order to avoid this problem, after each update some random, uniformly distributed samples are added to the set. These added samples are used in case the robot loses track of its position. The random samples uniformly distributed in the whole environment can effectively re-localize the robot. In case the position of the robot is not lost, the weight of these random samples will decrease and the samples will disappear in the next iteration.

(a) Initialization (b) Uncertainty due to symmetry (c) Final localization

Figure 2.3: Global localization of a robot using MCL

Figure 2.3 shows an example of a global localization performed by a robot using MCL. The first image shows the initial sample set distribution where the robot's position is unknown and the samples are uniformly distributed throughout the environment. The second image shows two probable robot positions after the robot has slightly moved; this uncertainty is caused by a symmetry in the map. The random samples in the second image are the ones added after each update. The third image shows the successful localization of the robot after it kept going forward. The information used to achieve this localization was the movement commands and the sensor information.

Nowadays, there are several programs that provide localization capabilities using simultaneous localization and mapping (SLAM). SLAM is the process of constructing a map of an unknown environment while keeping track of the agent's location in it. The agent is normally a robot or an autonomous vehicle.

In the next section, a new SLAM software will be presented: *Google Cartographer*. Google cartographer can obtain information from two different types of sensors, namely sonar and laser scanners, and can be implemented in virtually any mobile robot.

2.1.3 Google Cartographer

—— TODO: Enter some description here and explain it was used to create a map of the lab used to localize the robot. Gives better results than the previously used software ——

2.2 Kinematic Modelling of a Robot

According to Siciliano and Khatib [2008], *robot kinematics* refers to the motion of the elements in a robot without considering the forces and torques that generated this movement. To describe the movement of a robot, we need a kinematic model of its structure. The position and orientation of a body in space is known as *pose*.

A robot can be modeled as a kinematic chain, which consists of a system of rigid bodies connected by joints, a *kinematic joint* is a connection between 2 bodies that constrains their relative motion. In robotics, these bodies are usually referred to as *links*. The kinematic description of a robot normally uses some simplifications: the links that form the robot are assumed to be rigid, and each link is ideally connected with the next one, with no gap in between.

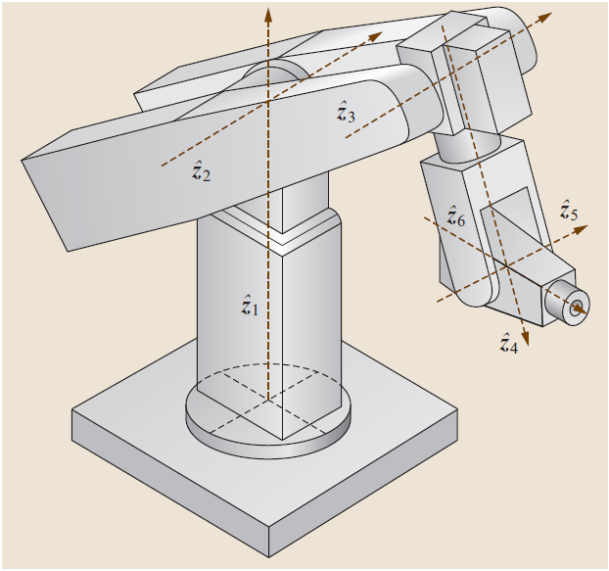

Figure 2.4: Example of a 6 DOF manipulator. [Siciliano and Khatib, 2008, chap. 1, page 24]

Figure 2.4 shows an example of a serial chain manipulator, where a reference frame is attached to each link. Following the Denavit-Hartenberg convention, the Z axis is always aligned with the joint axis [Craig, 2005].

The study of robot kinematics involve how the location of the reference frames change as the mechanism moves. The main goal is to compute the position and orientation of the manipulator's end-effector with respect to the base as a function of the joints values.

For an open-loop robotic mechanism, the general structure is represented by a kinematic tree, which consists of the concatenation of links and joints with a reference frame in each joint [Siliciano and Khatib, 2008]. This representation is used to obtain a mathematical model of the system.

When programming a robot, a suitable representation of its kinematic model is required. The Unified Robot Description Format (URDF) is a standard XML representation of the robot model in the ROS community[1], which includes the robot kinematics, dynamics, and sensors.

2.3 Collision Environment

The workspace of a robot is defined as the total volume swept out by the end-effector as the manipulator executes all possible motions [Siliciano and Khatib, 2008, chap. 1]. In simple terms, the workspace is the space that can be reached by the robot.

The working environment consists of all the external factors surrounding and affecting the robot. In other words, it is the space where the robot is working, including all the objects in there. According to Dmitry Berenson and and Kuffner [2011], the robot is considered to be operating

[1] http://wiki.ros.org/urdf

in a "world" that it cannot leave; actions can affect the environment and, thus, change it for the robot.

The environment can be represented in a graphical way with meshes that describe the geometry of the objects and of the robot. The position of the meshes in the model environment has to match the position of the real objects. Motion planning algorithms are then used to calculate trajectories that the robot can execute without colliding with the environment or itself.

A robot can have two types of sensors [Russell, 1990, chap. 1]:

- **Proprioceptive sensors:** Get information about the internal state of the robot, such as the angular position of each joint or the temperature of the links. These sensors are used for self maintenance and control of internal status. Examples of proprioceptive sensors are: shaft encoders, inertial navigation systems and force sensors.
- **Exteroceptive sensors:** Obtain information from the robot's environment, such as the distance to an object relative to a frame of reference of the robot. Many exteroceptive sensors are sensors that can be used to calculate distances. These sensors can be further categorized in contact, range, and vision sensors.

The robot takes the information from proprioceptive sensors to calculate the position and orientation of each link and determine its current configuration, and the information from exteroceptive sensors to calculate its position relative to the environment and the distance to surrounding objects. Combining both, the motion planning algorithms can iterate until a collision-free path between the initial and desired position is found.

2.4 Trajectory Planning

According to Han et al. [2011, chap. 1, page 6] *"A trajectory is the path that a moving object follows through space as a function of time"*. A trajectory can be described as a time-stamped series of location points.

To define a robot's trajectory, we must define the trajectory that each link will execute to bring the robot to a desired pose. Once the robot's kinematic model and environment are defined, we use a motion planning algorithm to solve the path planning problem and obtain a collision-free trajectory for the robot. Planning involves determining the path and the velocity function for a robot.

2.4.1 Euclidean Space in Cartesian Coordinates

In geometry, we can describe the position of any object in space using Cartesian coordinates (X, Y, and Z). For a 3-dimensional space (Euclidean space), any object can move and rotate along 3 axes, this means that the object has 6 degrees od freedom (DOF), so 6 values are required to define the pose of an object with respect to a reference point. In other words, for a three-dimensional Euclidean space, we can describe the position and orientation of any object using the Cartesian coordinates and three rotation angles.

2.4.2 Configuration Space (C-space)

A complete description of the robot's geometry and of the workspace is needed to solve the path planning problem. A *configuration* $\boldsymbol{q}$ specifies the location of every point of the robot's geometry.

The *configuration space*, where $\boldsymbol{q} \in \boldsymbol{C}$, is the space of all possible configurations [Siliciano and Khatib, 2008]. It represents all possible transformations that can be applied to the robot given its kinematics. The C-space gives an abstract way of solving the planning, the main advantage of this representation is that a robot can be mapped into the C-space as a single point, where the number of DOF of the robot is the dimension of the C-space. This is also the minimum number of parameters required to describe a configuration, so motion planning for the robot is equivalent to motion planning for the C-space.

During trajectory planning, one must consider several constraints involving the robot's pose. Since the allowed configurations of the robot are not known beforehand, the planning algorithm must find these valid configurations while planning. Finding these configurations is normally done through sampling, this process can become inefficient for complex environments.

2.4.3 Motion Planning Algorithms

One of the fundamental problems of robotics is to plan motions for complex bodies from an initial pose to a goal. As explained by Siliciano and Khatib [2008], the general path planning problem is computing a continuous free path for the robot between $\boldsymbol{q}_1$ and $\boldsymbol{q}_G$, given:

1. The robot's workspace $\boldsymbol{W}$
2. An obstacle region $\boldsymbol{O} \subset \boldsymbol{W}$
3. A robot defined as a collection of m links: $A_1, A_2, ..., A_m$
4. The C-space $\boldsymbol{C}$ with defined $\boldsymbol{C}_{obs}$ and $\boldsymbol{C}_{free}$
5. An initial configuration $\boldsymbol{q}_1 \in \boldsymbol{C}_{free}$
6. A goal configuration $\boldsymbol{q}_G \in \boldsymbol{C}_{free}$

Where C_{obs} is the *C-space obstacle region* and C_{free} is the set of configurations that avoid collision, called *free space*. We must compute a continuous free path for the robot between q_1 and q_G.

The main complication is calculating C_{obs} and C_{free}, that are needed to determine the region where the robot can move without colliding. There are two main approaches to solve the planning problem: sampling-based and combinatorial motion planning.

In this project, a controller developed at the Institute for Artificial Intelligence[2] (IAI), *Giskard* (section 2.5.3), will be used as robot motion controller.

Motion planners have several ways of approaching the problem and finding a suitable trajectory for the robot to execute. Some algorithms are: sampling-based motion planning and optimization based motion planning.

2.4.3.1 Sampling-based motion planning

The planner samples different configurations in the C-space to construct collision-free paths. These paths are stored as 1D C-space curves. The main idea is to avoid the direct construction of the obstacle region C_{obs}. This means that instead of considering the obstacles directly, the planner uses a collision detector for each pose in the trajectory. This approach allows using the planner for a wide range of applications, one must only adapt the collision detector to the geometry of a specific robot.

[2] http://ai.uni-bremen.de/

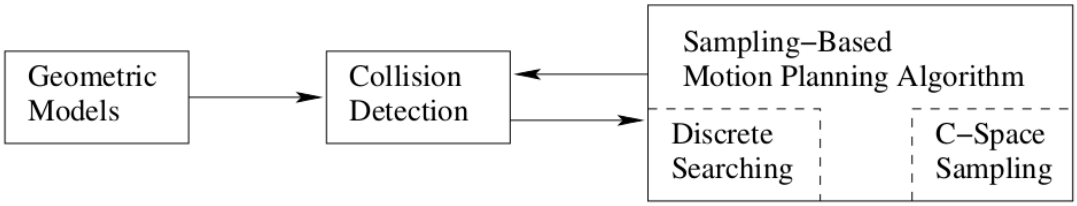

Figure 2.5: Sampling-based planning philosophy [LaValle, 2006, chap. 5, page 185].

The sampling-based planning, shown in figure 2.5, uses the collision detection as a "black box" between the motion planning and the geometric model of the robot. This generates an algorithm that is independent of the robot's geometry [LaValle, 2006] .

This "black box" approach can solve problems that involve thousands of geometric primitives representing the robot. It is practically impossible, according to Siliciano and Khatib [2008], to solve such problems with algorithms that uses the C_{obs} directly.

The disadvantage of these algorithms is that they don't assure to find a solution in a finite amount of time. Combinatorial motion planning algorithms are able to return a solution, if it exists, in a finite amount of time.

A **rapidly exploring random tree (RRT)** is a sampling-based planning algorithm that searches a collision-free path by randomly building a space-filling tree. It has a good performance and does not require any parameter tuning. As shown in figure 2.6, RRT reaches unexplored regions after just a few iterations.

Figure 2.6: Rapidly exploring random tree [LaValle, 2006, chap. 5, page 230].

The basic idea of RRT is to incrementally build a search tree in the C-space that tries to connect q_1 and q_G, avoiding the obstacles in the way, where G is the search graph. All the vertices of G are collision-free configurations.

RTT will try fo find a path in the tree that connects the starting point with the goal, thus generating a collision-free trajectory for the manipulator.

2.4.3.2 Optimization-based motion planning

TODO

Sample-based VS Optimization-based

2.5 Software

In the last years, the number of applications where humans and robots work in proximity to each other has increased. This has lead to the development of many software programs used for robot manipulation.

The institute for Artificial Intelligence (IAI) uses ROS to communicate with the robots, so this

project was done using ROS as base. For trajectory planning, I used Giskard (section 2.5.3), with RVIZ as a side tool for visualization.

2.5.1 ROS

Robot Operating System (ROS) is an open source software that helps developers to create robot applications. According to the official documentation[3], ROS is a meta-operating system, a system that handles other operating systems, it handles hardware abstraction, low-level device control, implementation of commonly-used functionality, message-passing between processes, and package management. ROS also provides a wide range of libraries and tools for robots, such as drivers and visualizers. Some of these libraries are focused on mobility, manipulation and perception tasks.

One of the ROS main components is its communication infrastructure. This has a message passing interface that provides inter-process communication and is seen as a middleware[4].

The communication consists of a publish/subscribe message passing system, where one program publishes information under a certain topic. All other programs subscribed to this topic will receive the information. A program can be sending information through one or more topics and, at the same time, receiving information from other topics. ROS works as the middleware that manages and distributes these messages.

ROS uses *nodes* to do computations. A node is a process that communicates with other nodes using topics and the parameter server. The main reason behind nodes is the simplification of program codes. A robot is controlled using many nodes, each one in charge of a small task, such

[3] http://wiki.ros.org/ROS/Introduction
[4] http://www.ros.org/core-components/

as localization or controlling a wheel; this breaks down the complexity of the system into many smaller subsystems (modules) that work independent of each other, communicating through topics and parameters.

Since most applications require several nodes to control all the subsystems, it is useful to have a code that can launch multiple nodes locally and remotely. A *launch file* is a XML configuration file with a *.launch extension, it can specify a set of parameters and nodes to launch. These files can also include other launch files.

2.5.2 RViz

RViz is a 3D visualization tool for ROS. RViz displays the sensor data and the robot's state information taken from ROS. Using RViz we can visualize the current state of the robot (figure 2.7), visualize simulated trajectories, and display information from the sensors, such as 3D point-clouds from the Kinect or the image obtained by a camera.

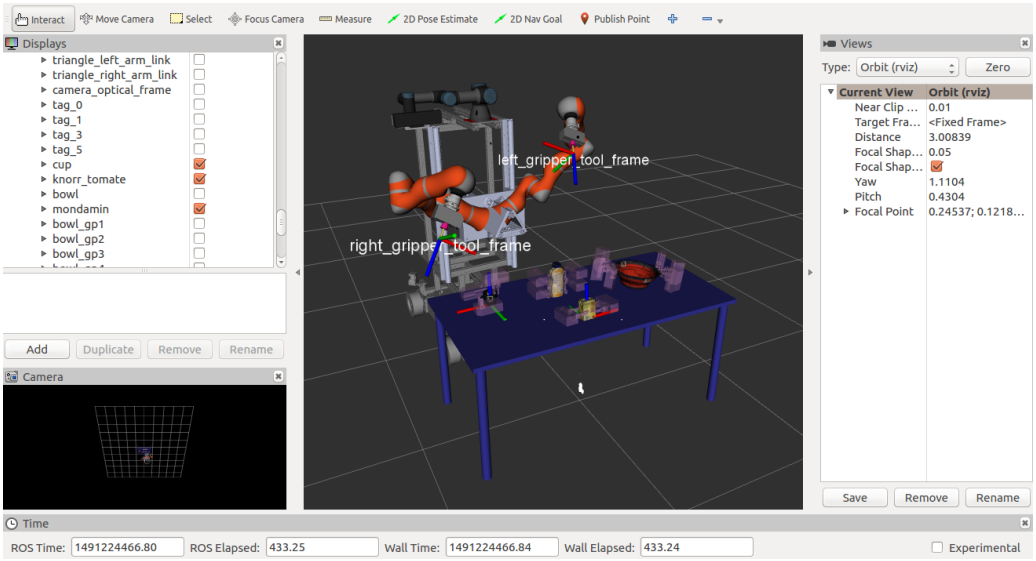

Figure 2.7: RViz visualization of Boxy.

RViz uses a *fixed frame* as a static reference for the visualization, the default frame is `\world`.

All the information that RViz receives is displayed with respect to this frame, including: robot's current state, location of objects in the environment, and data from sensors.

2.5.3 Giskard

2.5.4 Chili markers

2.6 Robot Description

In oder to calculate the position and movements of the robot, all it's elements must be represented in a way that the robot controller and the trajectory planner understands them. This implies models or descriptions where the geometry, movement ranges and kinematics are described. Such description is made with a Unified Robot Description Format (URDF).

As the name implies, a URDF is a file used to describe a robot, it contains XML specifications of the robot's geometry, kinematics, inertial, and sensing properties. It is the native robot description format in ROS. The URDF loads meshes that contains the geometry of one or several robot links and describes it's relative position with respect to the previous link, it also specifies the type and range of movement it has.

Instead of writing a URDF file, programmers normally write a XACRO of the file, a XACRO is a XML macro, which is easier to read and allows code reuse.

CHAPTER 3

Methodology

This chapter describes the general structure of the system and of all the elements that

3.1 Basics

The system developed in this work, which has the objective of allowing the robot to identify and grab a specified object, comprises several parts:

- **Object Database:** A database with a 3D model of the objects the robot will be able to grasp, as well as predefined grasping poses for each object.
- **Perception system:** In order to simplify the perception task, all objects are identified using markers. The position and orientation of the markers with respect to the reference frame of the objects is known.
- **Motion controller:** A constraint-based, optimization-based controller was developed. This controller allows the parametrization of the trajectory and automatically selects the better grasping pose according to the initial conditions.

A general description of the system's architecture is shown in figure 3.1. The system uses ROS (section 2.5.1) to send and receive information from the robot and the user, each rectangle

depicts a ROS node. All nodes communicate using ROS services, actions and messages.

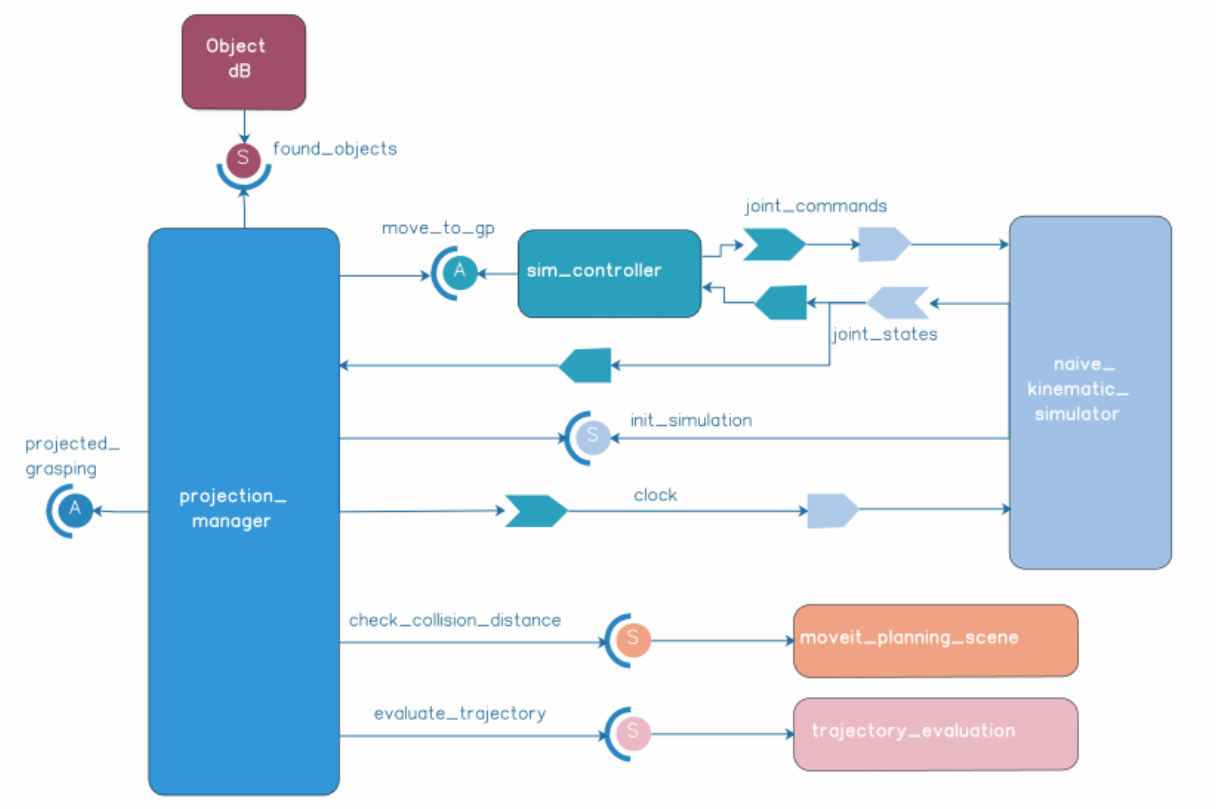

Figure 3.1: System architecture

The *Object dB* node is in charge of detecting objects and publishing it's current location, as well as the defined grasping poses for each object. The object's information is read from a YAML file (section 3.2.1). This node provides a service that publishes a list of found objects.

The component in charge of generating the trajectory is *sim_controller*, it receives the goal pose, calculates the required velocity for each joint and sends it to the *naive_kinematic_simulator*[1], which simulates the robot's movements.

The *projection_manager* node coordinates the whole system. It receives the request to grasp an object, asks the *Object dB* if the object was detected and requests the generation of a trajectory

[1] https://github.com/code-iai/iai_naive_kinematics_sim

to grasp it. Then, it sends the trajectories to the *trajectory_evaluation* noce, which evaluates between several proposed trajectories, selects one and sends it back as result.

3.2 Perception

The system requires previous knowledge about the objects the robot will interact with, it must be able to recognize the object and identify possible ways to grasp them. A 3D model of all objects was created, figure 3.2 shows an example of the models. These models are used for visualization in RVIZ.

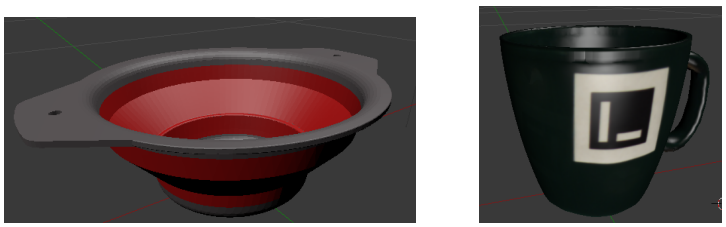

Figure 3.2: DAE models of a bowl and a cup. In the cup, one of the markers used for perception can be seen.

In order to simplify the perception task, markers were added to all objects. The markers used are Chilitags[2], which can be integrated with ROS[3]. Once the tags or markers are detected by the camera, it's position is published to a ROS topic. The *Object dB* node matches the corresponding objects to the found markers and displays the models in RVIZ.

3.2.1 Object Database

All the information about the objects is stored in a YAML file that works as database. The information is stored using the following structure:

[2]http://chili.epfl.ch/software
[3]https://github.com/chili-epfl/ros_markers

```yaml
object_name:
  id: 01                    # object ID number
  marker: [tag_1, tag_2]    # markers placed in the object
  tag_1:                    # Position and orientation of the markers with
                            # respect to the object frame of reference
    position: [0.003, 0.069, 0.03]
    orientation: [ 0.670,  0.016, -0.015,  0.741]
  tag_2:
    position: [0.005, 0.0678, 0.0345]
    orientation: [ 0.061,  0.740, -0.665,  0.068]
  mesh: package://iai_markers_tracking/meshes/object.dae  # 3D model
  scale: 1.0                # if the model is in cm = 1, m = 0.001
  gripper_opening: 0.0055   # how much the gipper should open to
                            # grasp the object
  grasping_poses:           # predifined grasping poses
    - p_id: gp1
      position: [0.058, 0.0, 0.048]
      orientation: [-0.70710678, 0.0, 0.0, 0.70710678]
    - p_id: gp2
      position: [0.058, 0.0, 0.048]
      orientation: [0.70710678, 0.0, 0.0, 0.70710678]
    - p_id: gp3
      position: [-0.036, -0.0, 0.06]
      orientation: [0, 1.0, 0.0, 0.0]
```

This structure is filled for every object the robot will grasp and added at the end of the YAML file.

3.2.2 Grasping Poses

For humans, it is intuitive how an object can be grasped, but for a robot it is not an easy task. In this project, grasping poses (GP) are already defined for each object, so that the robot only has to choose which pose to use in every situation.

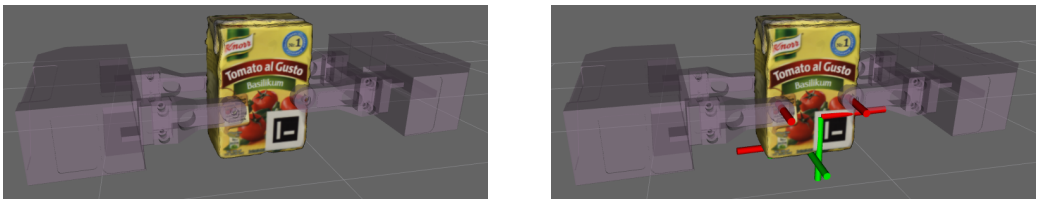

(a) (b)

Figure 3.3: 3D model of a tomato sauce package with two grasping poses. The object and GP have reference frames.

Figure 3.3 shows an object with two predefined GP. The perception system detects the position of the Chilitags markers, looks in the database for the corresponding object and GP and displays them in RVIZ, it also publishes a TF for both.

3.3 Motion Controller

The motion control system used to generate and control the movement of the robot is based on Giskard (section 2.5.3). Giskard uses *qpOASES*[4] to calculate a trajectory for each joint. As stated by Ferreau et al. [2014], qpOASES is an open-source optimization software that can solve quadratic programming (QP) problems of the form:

$$\min_x c(x) \;=\; \min_x \left(\frac{1}{2}\, x' \,\mathbf{H}\, x + x' \, g(\omega_0) \right) \tag{3.1}$$

Where $H \in \Re^{nV \times nV}$ is a symmetric and positive (semi-)definite Hessian matrix and $g \in \Re^{nV}$ is a gradient vector that depends on the parameter ω_0. The software tries to minimize the cost function $c(x)$. This minimization is subject to some constraints:

$$lb(\omega_0) \;\leq\; x \;\leq\; ub(\omega_0)$$

$$lbA(\omega_0) \;\leq\; \mathbf{A}x \;\leq\; ubA(\omega_0)$$

[4] `https://projects.coin-or.org/qpOASES`

where lb, $ub \in \Re^{nV}$ are the lower and upper constraint bound vectors of x, the matrix $\mathbf{A} \in \Re^{nC \times nV}$ is the constrain matrix with the lower and upper constraint boundary vectors lbA, $ubA \in \Re^{nV}$. Equality constraints can be achieved by setting equal upper and lower boundaries.

Several simple controllers were built and tested in order to understand the characteristics of the trajectories obtained using qpOASES. The controllers describe a two degree of freedom (DOF) linear manipulator. A state vector, $\vec{s} \in \Re^{nV}$, that describes the system is used as the variable to minimize of the cost function:

$$\vec{s} = [\, \dot{q}_0 \;\; \dot{q}_1 \;\; \varepsilon]^T \tag{3.2}$$

where $\dot{q}_0$ is the velocity of the first joint, $\dot{q}_1$ the velocity of the second joint and ε is a slack variable. Introducing this vector in the cost function and setting the gradient g to zero:

$$\min_{\vec{s}} c(\vec{s}) \;=\; \min_{\vec{s}} \left(\frac{1}{2}\, \vec{s}' \, \mathbf{H} \, \vec{s} \right) \tag{3.3}$$

with the minimization constraints given by:

$$\vec{lb}(t) \;\leq\; \vec{s} \;\leq\; \vec{ub}(t) \tag{3.4}$$

$$\vec{lbA}(t) \;\leq\; \mathbf{A}\vec{s} \;\leq\; \vec{ubA}(t) \tag{3.5}$$

We define different weights for each parameter of the state vector $\vec{s}$ by setting the H matrix to:

$$\mathbf{H} \;=\; diag(\vec{\omega})$$

with the weight vector $\vec{\omega} \in \Re^{nV}$. These weights allows us to prioritize the movement of one specific joint over the others, considering that the cost function for the 2 DOF controller from eq 3.3 is given by:

$$c(\vec{s}) \;=\; \frac{1}{2}\, \vec{s}' \, \mathbf{H} \, \vec{s} = \; \frac{1}{2}\, (\, \dot{q}_0{}^2 \omega_1 + \dot{q}_1{}^2 \omega_2 + \varepsilon^2 \omega_3) \tag{3.6}$$

The software will try to minimize the cost of solving the problem by setting a higher value for

the variables with a lower weight.

The result of this minimization problem is the velocity required by each joint to reach a goal position in a certain time. This can be set as an equality constraint:

$$error = q_{eef,des} - q_{eef} \tag{3.7}$$

$$error \leq \dot{q}_0 + \dot{q}_1 + \varepsilon \leq error \tag{3.8}$$

where $q_{eef,des}$ is the desired position of the end effector (EEF) and q_{eef} the current position of the EEF. The position error can be used as a velocity goal if we suppose that we want to cover the distance error un one time unit. Velocity constraints are also established for each joint:

$$-\dot{q}_{0,max} \leq \dot{q}_0 \leq \dot{q}_{0,max} \tag{3.9}$$

$$-\dot{q}_{1,max} \leq \dot{q}_1 \leq \dot{q}_{1,max} \tag{3.10}$$

The software will try to find the velocity required by each joint to minimize the position error in one time step. Since the joints have velocity limits, it might not be possible to set velocities that satisfy the constraint set by eq 3.8, that is why the slack variable ε was introduced, with the constraints:

$$-\varepsilon_{max} \leq \varepsilon \leq \varepsilon_{max} \tag{3.11}$$

where $\varepsilon_{max} \gg q_{0,max}, q_{1,max}$. The weight of the slack value is higher than the ones of the joint velocities, so the software will try to give a higher value to the velocities than to the slack variable.

The joint limits also have to be taken into consideration:

$$-q_{0,max} - q_0 \leq \dot{q}_0 \leq q_{0,max} - q_0 \tag{3.12}$$

$$-q_{1,max} - q_1 \leq \dot{q}_1 \leq q_{1,max} - q_1 \tag{3.13}$$

These constraints will reduce the joint velocities when they are approaching the limits until they reach zero at joint limit. The obtained velocity is the velocity the joints would have to instantaneously reach to get to the goal potion in one time instant. However, due to physical limitations, joints can not immediately reach maximum velocity on one time step, so acceleration limits have to be established:

$$-a_{0,max} \leq \dot{q}_0 \leq a_{0,max} \tag{3.14}$$

$$-a_{1,max} \leq \dot{q}_1 \leq a_{1,max} \tag{3.15}$$

Combining equations 3.8 to 3.15 to create the constraint bound vectors from equations 3.4 and 3.5, we obtain:

$$\begin{pmatrix} -\dot{q}_{0,max} \\ -\dot{q}_{1,max} \\ -\varepsilon_{max} \end{pmatrix} \leq \begin{bmatrix} \omega_1 & 0 & 0 \\ 0 & \omega_2 & 0 \\ 0 & 0 & \omega_3 \end{bmatrix} * \begin{pmatrix} \dot{q}_0 \\ \dot{q}_1 \\ \varepsilon \end{pmatrix} \leq \begin{pmatrix} \dot{q}_{0,max} \\ \dot{q}_{1,max} \\ \varepsilon_{max} \end{pmatrix} \tag{3.16}$$

$$\begin{pmatrix} error \\ -q_{0,max} - q_0 \\ -q_{1,max} - q_1 \\ a_{0,min\_lim} \\ a_{1,min\_lim} \end{pmatrix} \leq \begin{bmatrix} 1 & 1 & 1 \\ 1 & 0 & 0 \\ 0 & 1 & 0 \\ 1 & 0 & 0 \\ 0 & 1 & 0 \end{bmatrix} * \begin{pmatrix} \dot{q}_0 \\ \dot{q}_1 \\ \varepsilon \end{pmatrix} \leq \begin{pmatrix} error \\ q_{0,max} - q_0 \\ q_{1,max} - q_1 \\ a_{0,max\_lim} \\ a_{1,max\_lim} \end{pmatrix} \tag{3.17}$$

The constrains set by these equations are the groundwork for the basic controllers explained in the following subsections. All these cases simulate a translational 2 DOF system, the goal is to position the EEF at a given distance (goal). The initial position of each joint is given, as well as a goal for the EEF. The initial velocity of the joints is assumed to be zero, but other initial

conditions could also be set.

3.3.1 Simple 2 DOF controller

A proportional gain for the joints goal is introduced in order to reduce the number of iterations the program required to solve the problems. In other words, the proportional gain can be used to increase the joint velocities. Rewriting equation 3.7:

$$error = p * \left(q_{eef,des} - q_{eef}\right) \tag{3.18}$$

Figures 3.4 and 3.5 show the position and velocity of a 2 DOF manipulator, whose trajectory is calculated using equations 3.16 and 3.17 to obtain the joint velocity in each time step. Figure 3.4 shows the EEF position (blue), velocity (orange) and the goal position (green), while figure 3.5 shows the position and velocity of the joints q_0 and q_1.

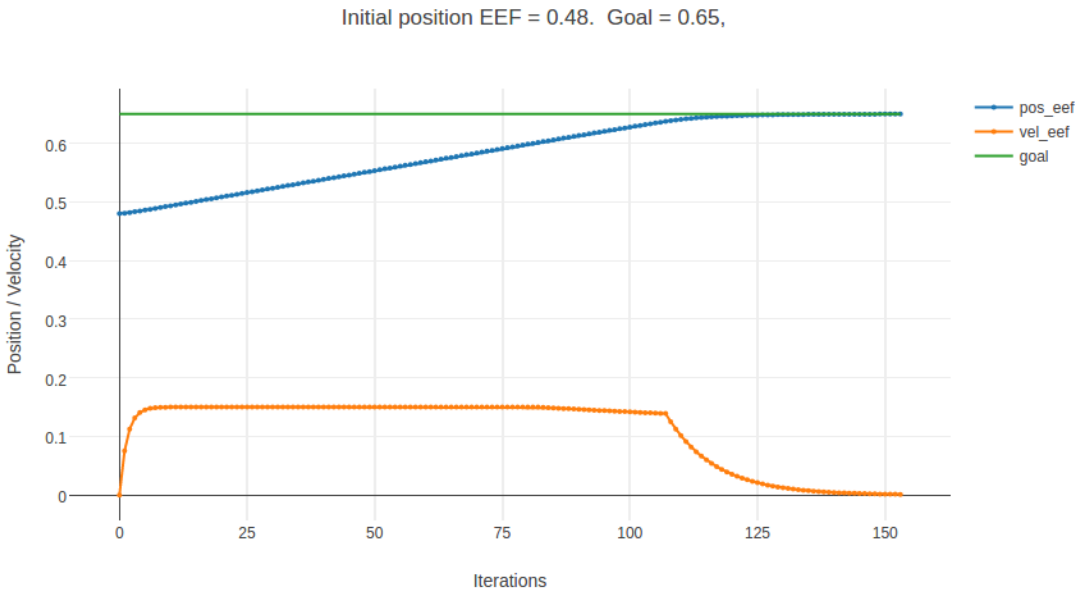

Figure 3.4: EEF trajectory. Initial acceleration is limited by constraints. Velocity decreases as EEF aproaches the goal position.

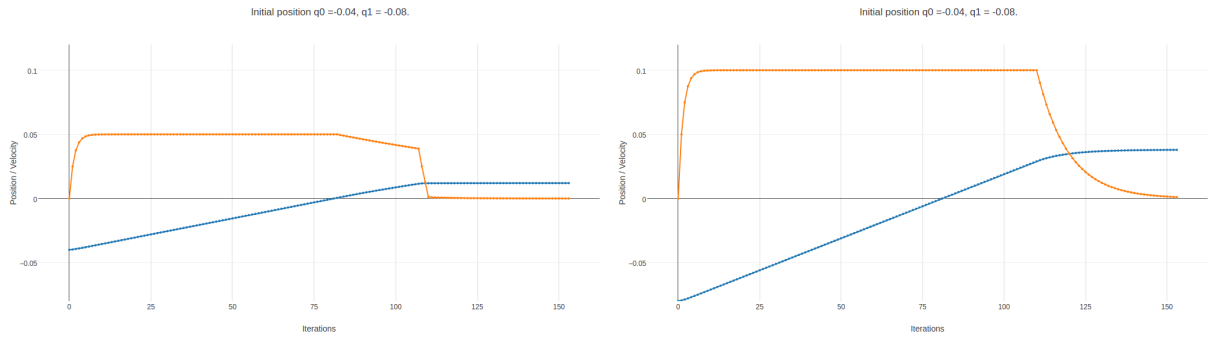

(a) Joint q_0 (b) Joint q_1

Figure 3.5: Joints trajectories (blue). Each joint has different velocity(orange) and acceleration constraints.

It can be seen that the velocity decreases once the EEF is approaching the desired position, also the joints do not reach the maximum velocity in the first time step. This is due to the acceleration constraint given by equations 3.14 and 3.15, the maximum acceleration is calculated on every iteration with:

$$a_{n,max\_lim} = \frac{\dot{q}_{n,max} - a_{n,max}}{\dot{q}_{n,max}} + a_{n,max} \tag{3.19}$$

$$a_{n,min\_lim} = \frac{\dot{q}_{n,max} - a_{n,max}}{\dot{q}_{n,max}} - a_{n,max} \tag{3.20}$$

where n is the joint number and $a_{n,max}$ a constant acceleration limit.

3.3.2 Joints goal and EEF goal

This example allows to specify a goal position for one of the joints as well as for the EEF. Figures 3.6 and 3.7 show the behavior of the EEF and both joints while reaching the specified goals. Each joint has different velocity and acceleration constraints.

In this controller, the weight vector is defined as $\vec{\omega} = [\omega_1,\ \omega_2,\ \omega_3,\ \omega_4]$. Where ω_1 and ω_2 are the joint weights, ω_3 is the weight of the slack factor and ω_4 is the weight of the joint goal.

Equation 3.17 is rewritten as:

$$\begin{pmatrix} error \\ -q_{0,max} - q_0 \\ -q_{1,max} - q_1 \\ a_{0,min\_lim} \\ a_{1,min\_lim} \\ joint\_error \end{pmatrix} \leq \begin{bmatrix} 1 & 1 & 1 & 0 \\ 1 & 0 & 0 & 0 \\ 0 & 1 & 0 & 0 \\ 1 & 0 & 0 & 0 \\ 0 & 1 & 0 & 0 \\ 1 & 0 & 0 & 1 \end{bmatrix} * \begin{pmatrix} \dot{q}_0 \\ \dot{q}_1 \\ \varepsilon \\ \varepsilon_j \end{pmatrix} \leq \begin{pmatrix} error \\ q_{0,max} - q_0 \\ q_{1,max} - q_1 \\ a_{0,max\_lim} \\ a_{1,max\_lim} \\ joint\_error \end{pmatrix}$$

Where ε_j is the slack factor for the joint goal and $joint\_error$ is the current error of the joint q_0 to the joint goal, given by $joint\_error = q_{0,des} - q_0$

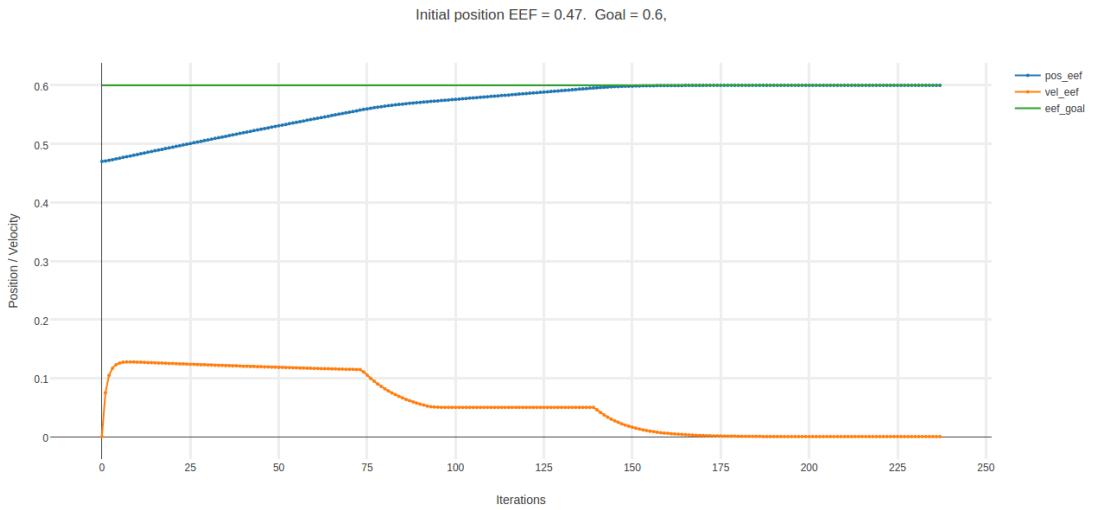

Figure 3.6: Trajectory (blue), velocity (orange) and goal (green) of the EEF.

The initial position ot the EEF is 0.47, and of the joints $q_0 = 0.02$ and $q_0 = -0.15$, respectively. Only a goal for the EEF and for the first joint, $EEF_f = 0.6$ and $q_{0f} = -0.25$. are specified.

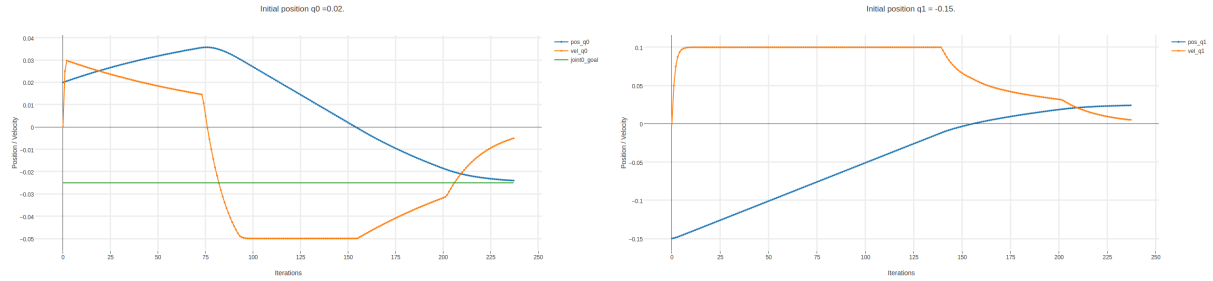

(a) Joint q_0 (b) Joint q_1

Figure 3.7: Trajectories (blue) and velocities (orange) of both joints and goal (green) of q_0.

It can be seen in figure 3.7 that one of the joints changes direction after around 75 iterations. This happens because the goal of the EEF and of the joint are in different directions, the system tries to minimize first the EEF error and afterwards the one of the joint. This behavior suggest that it might be better to split the problem when goals for the joints are specified, where in the first part the joint goals are satisfied and kept constant and in the second part the EEF is reached.

3.3.3 Position range as goal for the EEF

In this example, the goal specified for the EEF is not one specific position, but a range, where any point in this area is a valid goal for the EEF.

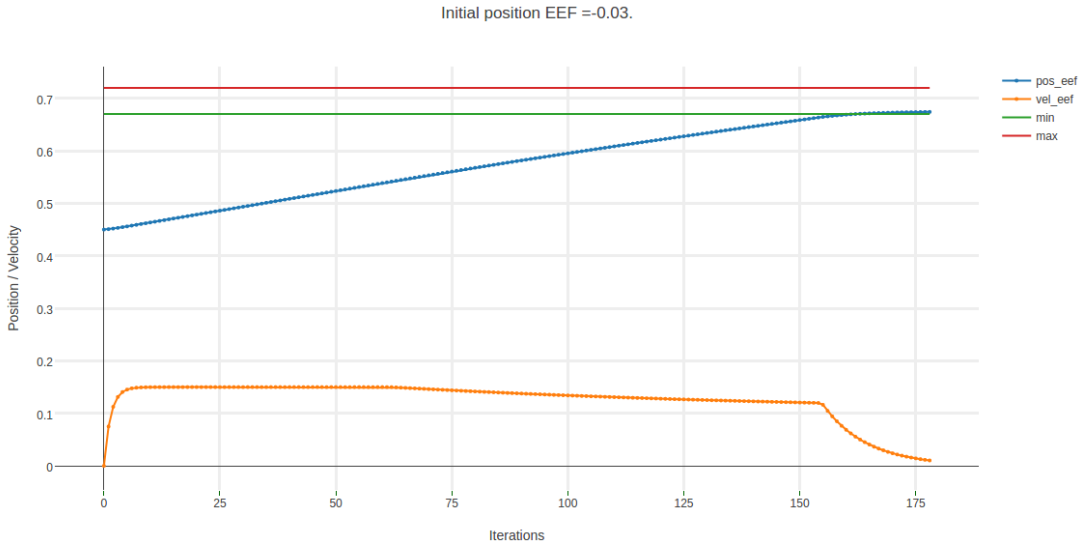

Figure 3.8: Trajectory (blue) and velocity (orange) of the EEF, the goal range is between the green and red lines.

Figure 3.8 shows the trajectory followed by the EEF while reaching the goal, it stops shortly after entering the given goal range. If a specific point inside this range is preferred as goal, an *attractor* can be created,so that the EEF will try to reach the point defined by the attractor, but, if it is not possible, it will stay in the goal range.

To achieve this behavior, matrix **A** and it's limits, $\vec{lbA}$ and $\vec{ubA}$, are modified, rewriting equation 3.17 as:

$$\begin{pmatrix} error \\ -q_{0,max} - q_0 \\ -q_{1,max} - q_1 \\ a_{0,min\_lim} \\ a_{1,min\_lim} \\ range_{min} - q_{eef} \end{pmatrix} \leq \begin{bmatrix} 1 & 1 & 1 & 0 \\ 1 & 0 & 0 & 0 \\ 0 & 1 & 0 & 0 \\ 1 & 0 & 0 & 0 \\ 0 & 1 & 0 & 0 \\ 1 & 1 & 0 & 1 \end{bmatrix} * \begin{pmatrix} \dot{q}_0 \\ \dot{q}_1 \\ \varepsilon \\ \varepsilon_r \end{pmatrix} \leq \begin{pmatrix} error \\ q_{0,max} - q_0 \\ q_{1,max} - q_1 \\ a_{0,max\_lim} \\ a_{1,max\_lim} \\ range_{max} - q_{eef} \end{pmatrix}$$

Where ε_r is the slack factor for the goal range, the error is calculated using the attractor (goal) $error = attr - q_{eef}$. Here, the weight vector is defined as $\vec{\omega} = [\omega_1,\ \omega_2,\ \omega_3,\ \omega_4]$. Where ω_1 and ω_2 are the joints weights, ω_3 is the weight of the attractor and ω_4 is the weight of the goal range. The constraints of the state vector (eq. 3.16) is rewritten as:

$$\begin{pmatrix} -\dot{q}_{0,max} \\ -\dot{q}_{1,max} \\ -\varepsilon_{max} \\ \varepsilon_{r,max} \end{pmatrix} \leq \begin{bmatrix} \omega_1 & 0 & 0 & 0 \\ 0 & \omega_2 & 0 & 0 \\ 0 & 0 & \omega_3 & 0 \\ 0 & 0 & 0 & \omega_4 \end{bmatrix} * \begin{pmatrix} \dot{q}_0 \\ \dot{q}_1 \\ \varepsilon \\ \varepsilon_r \end{pmatrix} \leq \begin{pmatrix} \dot{q}_{0,max} \\ \dot{q}_{1,max} \\ \varepsilon_{max} \\ \varepsilon_{r,max} \end{pmatrix}$$

Figures 3.9 to 3.10 show the behavior of the EEF and joints, in this example the attractor was set at 0.7, with the range between 0.67 and 0.72. It can be seen how the EEF reaches the goal set by the attractor, instead of just staying at the range borders.

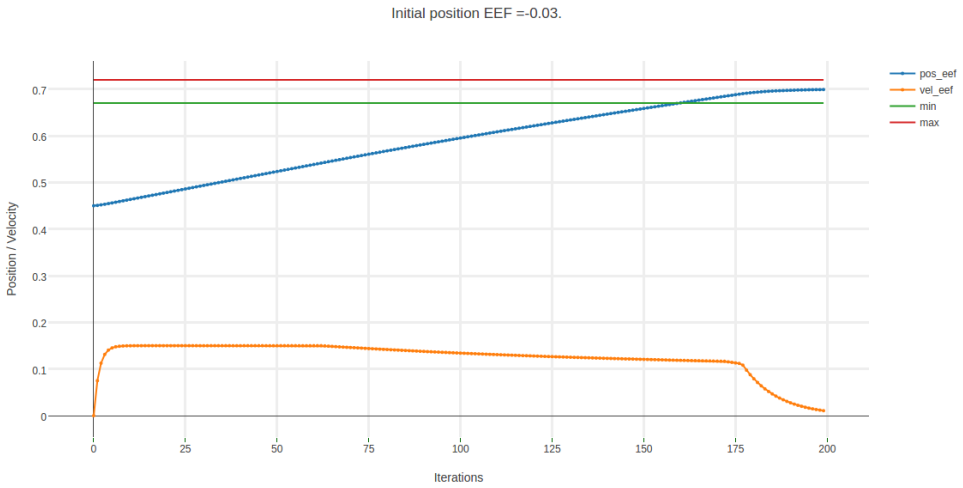

Figure 3.9: Trajectory (blue) and velocity (orange) of the EEF, here an attractor is defined inside the range.

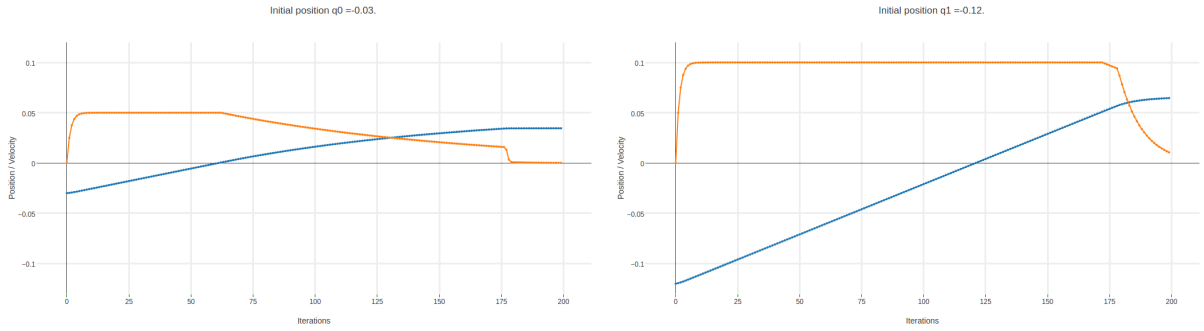

(a) Joint q_0 (b) Joint q_1

Figure 3.10: Trajectory (blue) and velocity (orange) of both joints. Each joint has a different velocity and acceleration constraint, as well as different joint limits.

The weight of the attractor is set higher than the range's weight, this means that the cost of reaching the point defined by the attractor is higher than just going inside the range. By doing this, the optimization algorithm prioritizes moving the EEF to the given range. Modifying these weights determine how close will the EEF come to the attractor.

3.3.4 Multiple goals for the EEF

It is also possible to specify multiple goals for the EEF and select them using the weights assigned to each goal. This controller shows a two DOF linear manipulator where twu goals are specified. In this case, the matrix $\mathbf{A}$ and it's limits (given by equation 3.17) is modified in the next way:

$$\begin{pmatrix} error_{goal1} \\ error_{goal2} \\ -q_{0,max} - q_0 \\ -q_{1,max} - q_1 \\ a_{0,min\_lim} \\ a_{1,min\_lim} \end{pmatrix} \leq \begin{bmatrix} 1 & 1 & 1 & 0 \\ 1 & 1 & 0 & 1 \\ 1 & 0 & 0 & 0 \\ 0 & 1 & 0 & 0 \\ 1 & 0 & 0 & 0 \\ 0 & 1 & 0 & 0 \end{bmatrix} * \begin{pmatrix} \dot{q}_0 \\ \dot{q}_1 \\ \varepsilon_1 \\ \varepsilon_2 \end{pmatrix} \leq \begin{pmatrix} error_{goal1} \\ error_{goal2} \\ q_{0,max} - q_0 \\ q_{1,max} - q_1 \\ a_{0,max\_lim} \\ a_{1,max\_lim} \end{pmatrix}$$

Where ε_1 and ε_2 are the slack factor for the first and second goals, respectively. The weight vector is defined as $\vec{\omega} = [\omega_1,\ \omega_2,\ \omega_3,\ \omega_4]$. Where ω_1 and ω_2 are the joints' weights, ω_3 and ω_4 are the goals' weight. The constraints of the state vector (eq. 3.16) is rewritten as:

$$\begin{pmatrix} -\dot{q}_{0,max} \\ -\dot{q}_{1,max} \\ -\varepsilon_{1,max} \\ \varepsilon_{2,max} \end{pmatrix} \leq \begin{bmatrix} \omega_1 & 0 & 0 & 0 \\ 0 & \omega_2 & 0 & 0 \\ 0 & 0 & \omega_3 & 0 \\ 0 & 0 & 0 & \omega_4 \end{bmatrix} * \begin{pmatrix} \dot{q}_0 \\ \dot{q}_1 \\ \varepsilon_1 \\ \varepsilon_2 \end{pmatrix} \leq \begin{pmatrix} \dot{q}_{0,max} \\ \dot{q}_{1,max} \\ \varepsilon_{1,max} \\ \varepsilon_{2,max} \end{pmatrix}$$

In the first example, two goals are specified but only the first one is selected using the goal's weights. Goal one. located at $q_{des1} = 0.55$, has a weight of $\omega_3 = 0.1$ and the second goal, located at $q_{des2} = 0.75$, has a weight of $\omega_4 = 0.001$, the initial position of the EEF is at $q_{eef} = 0.7$. As shown in figure 3.11(a), the EEF reaches the first goal (red line).

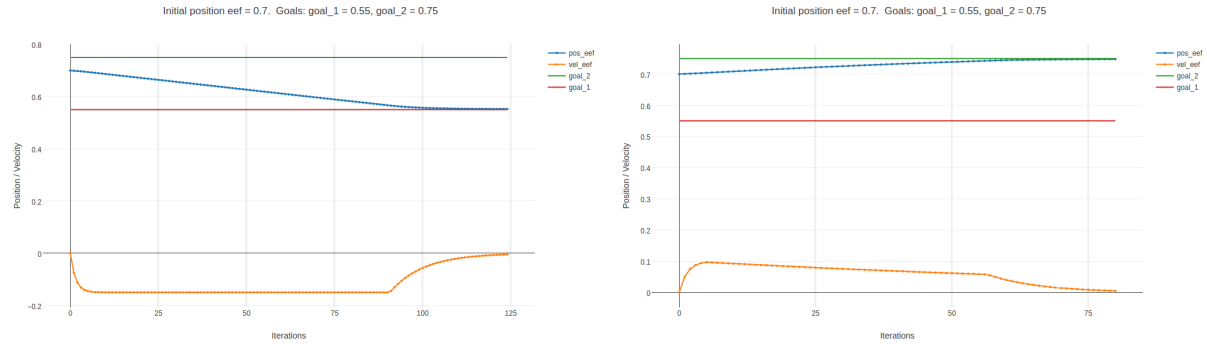

(a) First Goal (b) Second goal

Figure 3.11: The selected goal changes depending on the weights. Trajectory (blue) and velocity (orange) of the EEF.

By inverting the weights, $\omega_3 = 0.001$ and $\omega_4 = 0.1$, the active goal also changes (figure 3.11 (b)). It can be seen that the velocity of the EEF in figure 3.11 (b) is lower than in (a). This is caused due to the proximity of one of the joints to the joint limit, which was reached shortly after 50 iterations.

It is possible to make the EEF reach a point between both goals, by setting similar or equal weights to both goals (figure 3.12).

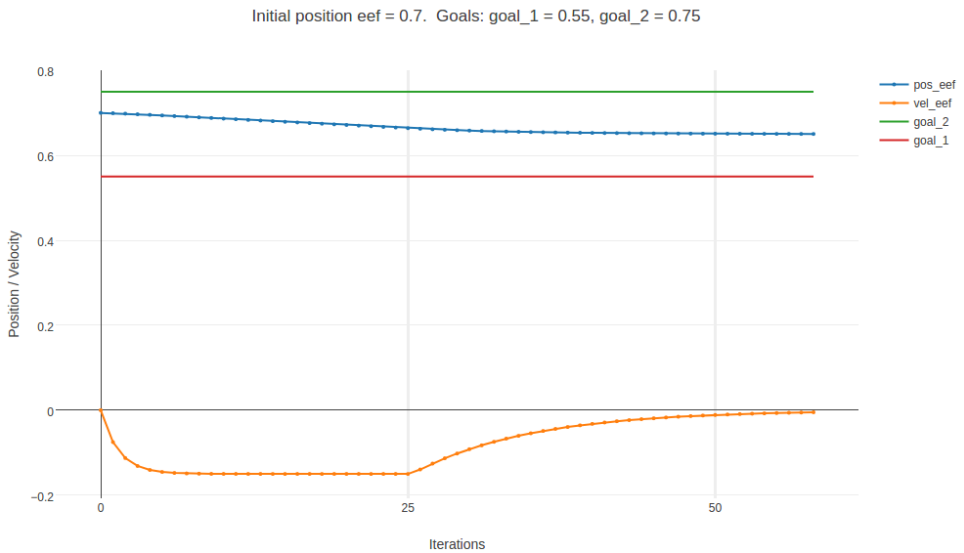

Figure 3.12: Trajectory (blue) and velocity (orange) of the EEF. Same weight in both goals. Each joint has a different velocity and acceleration constraint, as well as different joint limits.

If the weights of both goals is similar, the EEF will stay closer to one of the goals. Selecting the appropriate weight combination, it is possible to reach any point between both goals.

3.3.5 Dynamic weights

It is also possible to automatically select between two goals using dynamic weights, which change with the distance. This controller calculates the goals' weight in every iteration, with the error to the goals q_{des1} and q_{des2} as:

$$error_1 = (q_{des1} - q_{eef}) * p \qquad error_2 = (q_{des2} - q_{eef}) * p$$

where p is the proportional gain and q_{eef} the current position of the EEF. The weights are calculated with:

$$\omega_3 = \frac{error_2}{error_1 + error_2}^2 \qquad \omega_4 = \frac{error_1}{error_1 + error_2}^2 \tag{3.21}$$

The controller will then go to the closest goal, which gets a higher weight. In this example, the initial position of the EEF is set between both goals. As shown in figure 3.13, the EEF reaches the closes goal.

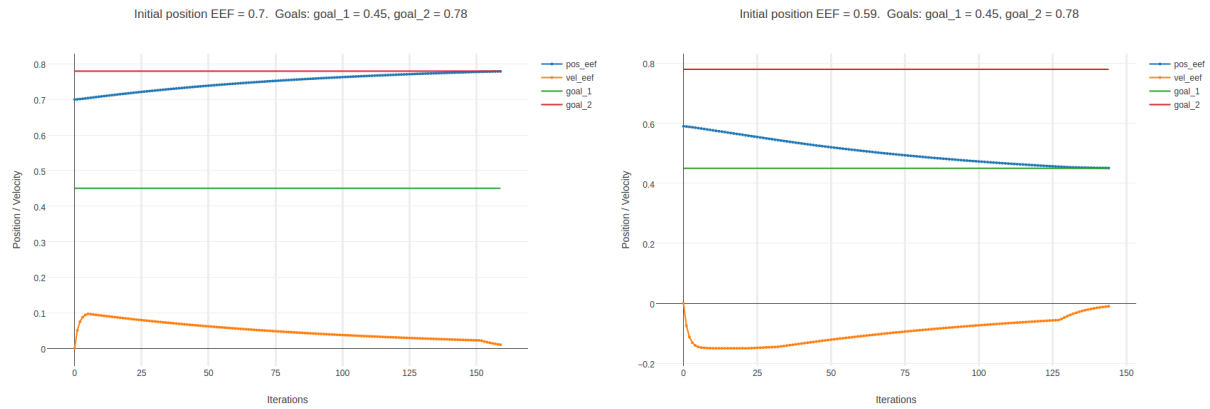

(a) EEF closer to goal 2 (red)

(b) EEF closer to goal 1 (green)

Figure 3.13: The selected goal changes depending on the initial position of the EEF, weights are calculated on every iteration. Trajectory (blue) and velocity (orange) of the EEF.

The only parameter changed between figure 3.13 (a) and (b) is the EEF's initial position.

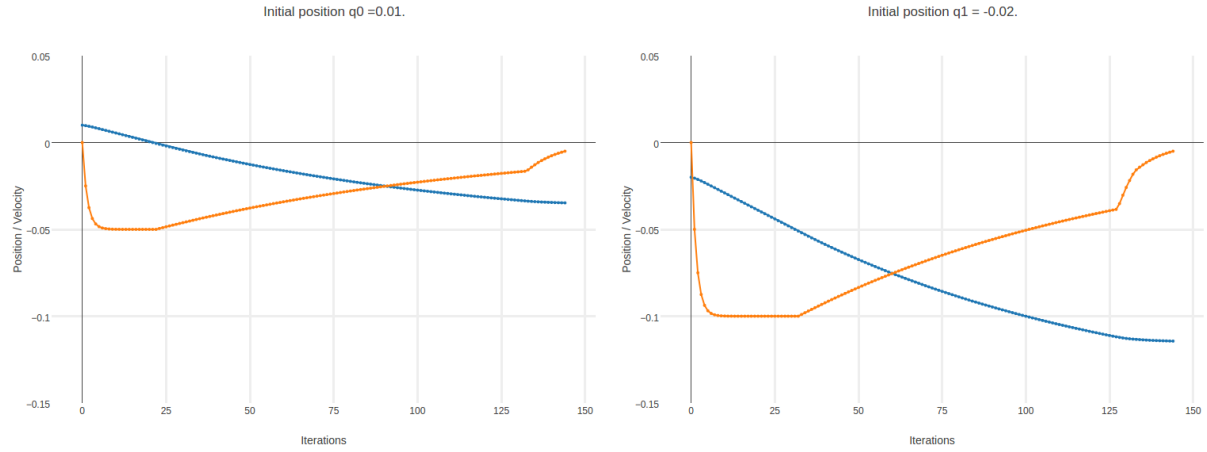

(a) Joint q_0 (b) Joint q_1

Figure 3.14: Trajectories (blue) and velocities (orange) of both joints. Each joint has a different velocity and acceleration constraint, as well as different joint limits.

Figure 3.14 shows the trajectories followed by both joints in the second example (3.13 (b)). It can be seen that the velocity profile oc both joints is similar. The different scale is due to the velocity constraints each joint has.

3.3.6 Three goals for the EEF

A problem seems to appear if dynamic weights are calculated when three or more goals are specified. Taking three goals as an example, if two of them are close together (q_{des2} and q_{des3}), the controller will ignore the third goal (q_{des1}) and reach for a point between the other goals, since minimizing two errors is better (mathematically speaking) than one.

This problem can be solved by modifying the formula used to calculate the goal's weights, so we can rewrite equation 3.21 as:

$$\omega_3 = \frac{1 - |error_1 - error_{min}|^3}{error_{max} + error_{min}}$$

$$\omega_4 = \frac{1-|error_2 - error_{min}|}{error_{max} + error_{min}}^3$$
$$\omega_5 = \frac{1-|error_3 - error_{min}|}{error_{max} + error_{min}}^3 \tag{3.22}$$

where:

$$error_{min} = min(|error_1|, |error_2|, |error_3|)$$

$$error_{max} = max(|error_1|, |error_2|, |error_3|)$$

The matrix **A** and it's limits as well as the state vector are extended to fit the extra goals:

$$\begin{pmatrix} error_1 \\ error_2 \\ error_3 \\ -q_{0,max} - q_0 \\ -q_{1,max} - q_1 \\ a_{0,min\_lim} \\ a_{1,min\_lim} \end{pmatrix} \leq \begin{bmatrix} 1 & 1 & 1 & 0 & 0 \\ 1 & 1 & 0 & 1 & 0 \\ 1 & 1 & 0 & 0 & 1 \\ 1 & 0 & 0 & 0 & 0 \\ 0 & 1 & 0 & 0 & 0 \\ 1 & 0 & 0 & 0 & 0 \\ 0 & 1 & 0 & 0 & 0 \end{bmatrix} * \begin{pmatrix} \dot{q}_0 \\ \dot{q}_1 \\ \varepsilon_1 \\ \varepsilon_2 \\ \varepsilon_3 \end{pmatrix} \leq \begin{pmatrix} error_1 \\ error_2 \\ error_3 \\ q_{0,max} - q_0 \\ q_{1,max} - q_1 \\ a_{0,max\_lim} \\ a_{1,max\_lim} \end{pmatrix}$$

Two examples in figure 3.15 show the behavior of this controller

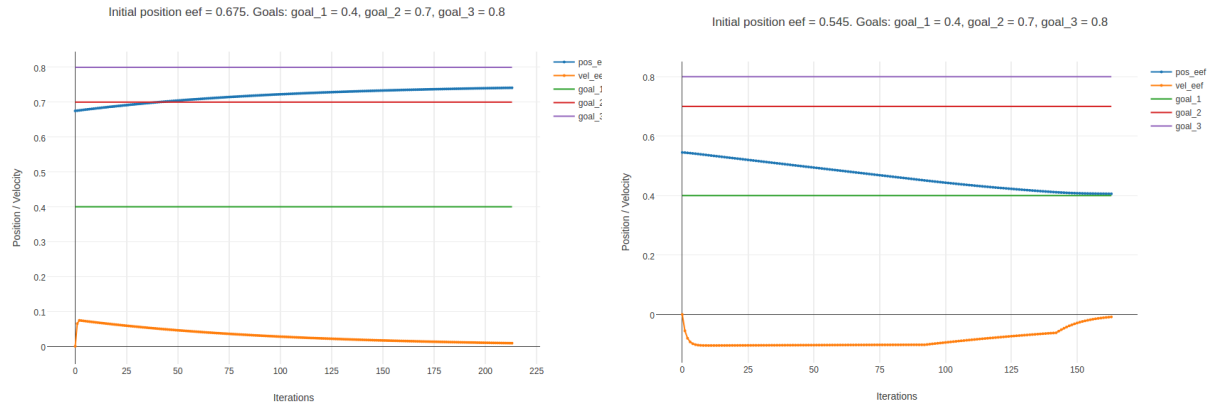

(a) EEF closer to goals 2 (red) and 3 (purple)

(b) EEF closer to goal 1 (green)

Figure 3.15: The selected goal changes depending on the initial position of the EEF. Trajectory (blue) and velocity (orange) of the EEF.

The controller does not always reach a goal, as seen in figure 3.15 (a), if two of the given goals are close together, the EEF will stay between both.This can still be implemented as a controller for a robot if the goals are grasping poses of an object, since the gripper will still reach out for the object.

The code of this controllers can be downloaded from Github[5].

3.3.7 Robot controller

A controller with the same structure as the ones showed in the previous subsections was developed for the Boxy robot. Boxy's geometry and kinematics are taken from the URDF file (section 2.6).

The definition of the matrix $\mathbf{A}$ and of the state vector $\vec{s} \in \Re^{nV}$ changes due to the DOF's and kinematics of the robot, so equation 3.2 changes to:

$$\vec{s} = [\ \dot{q}_0\ \ \dot{q}_1\ ...\dot{q}_C\ \ \varepsilon_0 ... \varepsilon_6]^T \tag{3.23}$$

where $\dot{q}_0$ to $\dot{q}_C$ are the joints velocities, three for the base, one for the torso and seven for the arm, and ε_0 to ε_6 are slack variables, one per DOF. The matrix $\mathbf{A} \in \Re^{nC \times nV}$ is defined using the Jacobian:

$$\mathbf{A} = \begin{bmatrix} \mathbf{J} & \mathbf{I}_{p,p} \\ \mathbf{I}_{m,m} & \mathbf{0}_{m,p} \\ \mathbf{I}_{m,m} & \mathbf{0}_{m,p} \end{bmatrix} \tag{3.24}$$

where $\mathbf{J} \in \Re^{p \times m}$ is the Jacobian, p is the number of DOF and m the number of joints to control.

[5] https://github.com/mgvargas/qpOASES

The constraint vectors are created using the error, joint limits and acceleration constraints:

$$\vec{lbA} = [\, \vec{error},\ -\vec{q}_{max} - \vec{q},\ \vec{a}_{min\_lim}]$$

$$\vec{ubA} = [\, \vec{error},\ \vec{q}_{max} - \vec{q},\ \vec{a}_{max\_lim}]$$

where the acceleration limit is calculated using equations 3.20 and 3.19, $\vec{q}_{max}$ is the vector of joint limits and $\vec{q}$ the current position of the joints.

The weight vector $\vec{\omega}$ is calculated on every iteration. If the robot is too far away from the given goal, the arm joints are disabled and only the base moves. Between a certain distance threshold, both base and arms can move, with the weights dynamically changing in accordance to the distance. If the robot is close to the goal, then only the arms and torso are allowed to move.

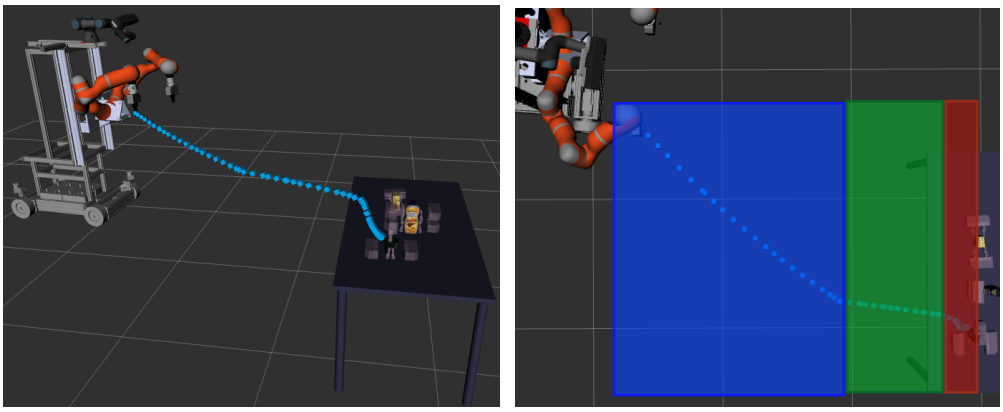

(a) Isometric view (b) Top view

Figure 3.16: Trajectory (blue) of the EEF. The weights are calculated on every iteration.

Figure 3.16 shows a simulated trajectory followed by the EEF while reaching out for a cup. The blue area in figure 3.16 (b) shows the part of the trajectory where only the base was moved, the green area is where arms, torso and base were active and the red area is where only the arms and torso were used.

3.4 Hardware and Software requirements

This project was developed in a computer running on Ubuntu 14.04, no special hardware is required to execute the generated code.

However, the user needs to have some programs and packages installed:

- **ROS:** With a configured workspace. The ROS distro used was *indigo*
- **MoveIt!:** Requires previous installation of ROS
- **UR3 driver:** A recommended one is `ur_modern_driver`
- **Boxy repositories:** The `iai_boxy` and `iai_robots` from the IAI github repository[6]
- **UR3 MoveIt configuration:** The code generated as a result of this project[7]

After installing ROS and MoveIt!, the user has to download the specified repositories from Github.

[6] `https://github.com/code-iai`
[7] `https://github.com/mgvargas/Moveit_config`

APPENDIX A

Appendix

A.1 Github Repositories

Here you can find all the Github repositories with the code required to run this project.

- Code generated during this project:

  `https://github.com/mgvargas/iai_markers_tracking`

  `https://github.com/mgvargas/qpOASES`

- Boxy's model and description:

  `https://github.com/code-iai/iai_robots`

- Robot controller and simulator:

  `https://github.com/SemRoCo/giskard_examples`

  `https://github.com/airballking/iai_boxy_sim`

A.2 Code Execution

A.2.1 Perception system

A.2.2 Robot

A.2.2.1 Target: Single Goal (or One-hand grasping)

A.2.2.2 Target: Multiple goals (or Two-hand grasping)

Bibliography

John J. Craig. *Introduction to Robotics; Mechanics and Control*. Pearson Education International, third edition, 2005.

Siddhartha Srinivasa Dmitry Berenson and and James Kuffner. Task space regions: A framework for pose-constrained manipulation planning. *The International Journal of Robotics Research*, 32:1435–1460, 2011.

H.J. Ferreau, C. Kirches, A. Potschka, H.G. Bock, and M. Diehl. qpOASES: A parametric active-set algorithm for quadratic programming. *Mathematical Programming Computation*, 6(4):327–363, 2014.

Dieter Fox, Wolfram Burgard, Frank Dellaert, and Sebastian Thrun. Monte carlo localization: Efficient posotion estimation for mobile robots. *National Conference on Artificial Intelligence*, 16, 1999a.

Dieter Fox, Wolfram Burgard, and Sebastian Thrun. Markov localization for mobile robots in dynamic environments. *Artificial Intelligence Research*, 11:391–427, 1999b.

Jiawei Han, Yu Zheng, and Xiaofang Zhou. *Computing with Spatial Trajectories*. Springer, 2011.

Steven M. LaValle. *Planning Algorithms*. Cambridge, 2006.

R. A. Russell. *Robot Tactile Sensing*. Prentice Hall, 1990.

Bruno Siciliano and Oussama Khatib. *Springer Handbook of Robotics*. Springer, 2008.